Rare Metal Materials and Engineering
Volume 51, Issue 5, May 2022
Available online at www.rmme.ac.cn

Science Press

Cite this article as: Wang Ben, Wang Yufeng, Zhao Hua, et al. Effects of Cutting Temperature on CFRP Subsurface in Drilling Process[J]. Rare Metal Materials and Engineering, 2022, 51(05): 1613-1619.

ARTICLE

Effects of Cutting Temperature on CFRP Subsurface in Drilling Process

Wang Ben[1], Wang Yufeng[2], Zhao Hua[2], Wang Minghai[1]

[1] School of Mechatronics Engineering, Shenyang Aerospace University, Shenyang 110136, China; [2] Key Laboratory of Fundamental Science for National Defence of Aeronautical Digital Manufacturing Process, Shenyang Aerospace University, Shenyang 110136, China

Abstract: The effect of cutting temperatures on the hole quality in multi-layered carbon fibre reinforced polymer (CFRP)/Ti stacks was investigated. The cutting force, cutting heat, hole surface, and subsurface quality of CFRP during drilling with and without Ti alloy supporting layer were analyzed, and the evaluation method for subsurface damage was proposed. The results show the cutting temperature and subsurface quality are greatly influenced by the existence or absence of Ti alloy supporting layer, whereas the cutting force and surface quality are slightly affected. A large amount of cutting heat is generated during cutting process of CFRP and Ti alloy simultaneously, resulting in the significant increase in temperature at the exit part of CFRP holes. The high temperature reduces the rigidity and bonding performance of CFRP resin matrix, leading to serious subsurface damage of the fibre layers around the exit part of CFRP holes. The subsurface damage was also evaluated by the proposed method, and the fibre layer at the exit part of holes is the most damaged, and the farther the distance away from the exit part of holes, the less damaged the subsurface. Therefore, the cutting temperature significantly influences the subsurface quality of CFRP hole during the drilling of multi-layered CFRP/Ti stacks, and subsurface damage is crucial to evaluate the machining quality of CFRP.

Key words: drilling; CFRP/Ti stacks; subsurface quality; temperatures; damage evaluation

The carbon fibre reinforced polymer (CFRP) is widely used in aeronautics, military, medical treatment, and transportation fields due to its characteristics of lightweight, high modulus, high intensity, fair corrosion resistance, and good fatigue resistance[1-5]. During the assembly, CFRP structural components are connected locally to the Ti alloy supporting structure through bolts, forming the composite CFRP/Ti stacks. Therefore, the holes are required to drill on the composite CFRP/Ti stacks for strongly-bolted CFRP/Ti stacks.

Conventional drilling is a commonly used borehole technique. However, the high cutting force[6], high torque, serious tool wear[7], layering of composites[8], and poor hole quality[9] all restrict the drilling of CFRP/Ti stacks. The processing strategies for CFRP component and CFRP/Ti stacks have been studied. Wang et al[10] discussed the impact of drilling process parameters on axial forces and layering in CFRP drilling process, and found that the drilling applies a great axial force on the first processing section and affects CFRP layering. Xu et al[11] established an axial force distribution model for all CFRP drilling periods to investigate the superimposed effects of axial forces during drilling processing. Variations in axial force during a single rotation of drilling can be determined accurately, and the relationship between the axial force distribution and the drilling-induced damage locations is reported. Geng et al[12] investigated the effects of high temperature on the drilling process of CFRP/Ti stacks, and found that the friction between high-hardness cutting and the hole wall can reduce the accuracy of hole diameter and the hole wall quality. However, such influence can be ameliorated by decreasing the feed rate. It is also reported that the Ti alloy supporting layer can effectively inhibit the layering phenomenon at the exit part of holes in components.

During the drilling of CFRP and CFRP/Ti stacks, the severe

Received date: May 25, 2021
Foundation item: National Natural Science Foundation of China (51875367, 51505302); China Postdoctoral Science Foundation (2020M670790); Shenyang Youth Science and Technology Innovation Project (RC190072); Natural Science Foundation of Liaoning Province (2020-MS-234); Foundation of Liaoning Educational Committee (JYT2020004)
Corresponding author: Wang Ben, Ph. D., Professor, School of Mechatronics Engineering, Shenyang Aerospace University, Shenyang 110136, P. R. China, Tel: 0086-24-89728447, E-mail: wangben211@163.com

machining damage occurs inevitably, and the hole quality should be considered. Luo et al[13] established a model about the drilling force and deformation of CFRP/Ti stacks with low-rigidity to investigate the damage on laminated interfaces. Based on the orthogonal cutting, Xu et al[14] studied the cutting removal modes of CFRP/Ti stacks during drilling process, and found that the subsurface damage is increased with increasing the cutting angle. Ti alloy cuttings can scratch the hole walls of CFRP, which seriously influences the quality of hole surface. Tsao et al[15] investigated the effect of supporting structure on layering damage during the drilling process and proposed a theoretical model associated with cutting forces. Hrechuk et al[16] demonstrated an evaluation method for CFRP hole quality to clarify the physical damage caused by layering and uncut fibres, and constructed four standards of hole damages. In addition, an approximate linear relationship between the hole quality and tool wear is also determined.

Typical drilling environments are relatively closed, so the cutting zone temperature rises quickly and can become even higher than the glass transition temperature (GTT) of CFRP. Then, the damage near the exit part of CFRP holes occurs easily[17], including the damage of surface integrity and the engine body[18]. Sorrentino et al[19] proposed a sensing system for the temperature measurement of cutter and instrument during CFRP drilling process, and provided useful information to predict the distribution of cutting temperature on the laminated CFRP plate for damage reduction. Fu et al[20] revealed that the temperature distribution at the exit part of holes is related to the properties of CFRP materials and drilling conditions, such as depth and fibre cutting angle. In addition, the relationships among the maximum drilling temperature, position, and drilling depth are determined by recognizing the potential heat-affected zone (HAZ) according to the visual temperature characteristics.

Currently, the drilling of CFRP or CFRP/Ti stacks has been widely studied in terms of drilling processing parameters, damage at the entrance and exit of holes, and damage at the lamination interface. However, the cutting temperature and its effect on the subsurface quality of CFRP hole in CFRP/Ti stacks during drilling are rarely investigated. Hence, the effect of cutting temperature and cutting force on CFRP subsurface damages of CFRP/Ti stacks during drilling was analyzed in this research. A comparative study of CFRP drilling with and without Ti alloy supporting layer was conducted. A subsurface damage evaluation method was proposed and the subsurface damage distribution could be determined. This research provides reference and guidance for subsurface quality and damage analyses during drilling.

1 Experiment

The orientation angles of CFRP in this research were 0°, 45°, 90°, −45°, −45°, 90°, 45°, and 0°, and the stack thickness was 2 mm. The material parameters are listed in Table 1. The Ti-6Al-4V alloy with the thickness of 5 mm was used as the Ti alloy supporting layer. A hard alloy driller with a nominal diameter of 6 mm was used as the cutter.

A VMC850B numerical control process centre was used. The coolants were not used in this research to eliminate the influence of cooling liquid. The Ti alloy supporting layer can increase the quality of the exit part of holes in the composite during the drilling of CFRP/Ti stacks. Therefore, the drilling of CFRP and CFRP/Ti stacks, namely Process I and Process II, respectively, was conducted. Process I included the pretreatment of a through-hole of Φ6 mm in the Ti alloy plate. Then CFRP plate was placed on the Ti plate and machined under the same conditions as the pretreatment of Ti plate, i.e., the drilling without Ti alloy supporting layer was conducted in Process I (Fig.1a). Process II included the drilling of CFRP/Ti stacks in a single process, namely the drilling with Ti alloy supporting layer (Fig. 1b). The drilling parameters are shown in Table 2. Seven groups of tests in total were conducted in this research.

In the experiment, a Kistler9257B three-way dynamometer and Kistler 5070 charge amplifier were used to measure the cutting forces. Data collected by a data acquisition card were processed by DynoWare signal processing software. The cutting temperatures were estimated by a FLIR T630sc thermal infrared imager. There was a distance of 0.5 mm between the hole wall and the workpiece edges, and the thermal infrared imager lens and workpiece had a distance of 500 mm.

After drilling, CFRP plates were ground and polished by sandpapers (800#, 1000#, 1500#) and diamond polishing suspension for the morphology observation of the subsurface of hole walls.

2 Results and Discussion

2.1 Cutting force

Cutting forces in the machining process are normally evaluated by the forces F_x, F_y, and F_z. F_z mainly influences the quality at the entrance and exit parts of holes, while the torques M_x and M_y, generated by F_x and F_y, respectively, can cause deformation of the cutter, thereby triggering the vibrations. Hence, the hole diameter, the circular degree, and roughness of the cutter are all impacted[21]. Since CFRP used in this research is isotropic, the performance along x and y directions is basically the same; hence, M_x and M_y are basically the same. Due to the symmetry in M_x and M_y, this study only focuses on F_z and M_x during processing. The F_z and M_x values of CFRP drilling with and without Ti alloy supporting layer are shown in Fig. 2. The cutter begins to process the Ti alloy, as indicated by the zone D in Fig.2a and

Table 1 Physical properties of CFRP

Tensile strength/GPa	Young's modulus/GPa	Compressive strength/MPa	Shearing strength of internal plane/MPa	Bending strength/MPa
2.3	120	1410	90	1450

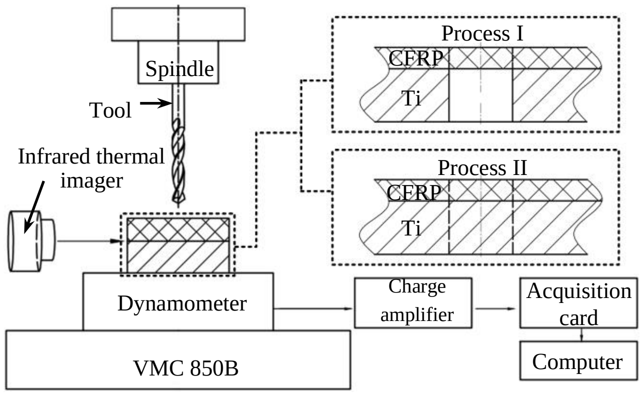

Fig.1 Schematic diagram of drilling processes

Table 2 Drilling process parameters

Tool speed, n_{tool}/ r·min^{-1}	Tool diameter, d_t/ mm	Feed rate, V_c/ mm·min^{-1}
1500	6	25

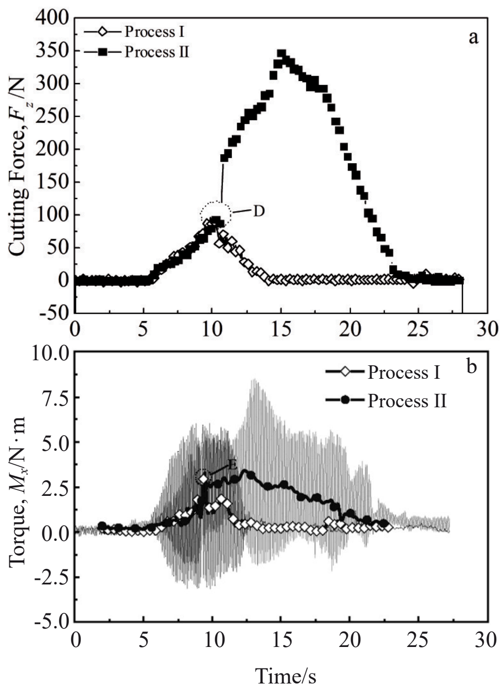

Fig.2 Cutting forces (a) and torques (b) of CFRP drilling with and without Ti alloy supporting layer

zone E in Fig.2b, resulting in a significant increase in cutting force. However, this study mainly focuses on stresses in CFRP. Thus, the subsequent cutting forces and torques after zone D and zone E are neglected.

The maximum F_z is 92.5 and 88.4 N and the maximum M_x is 3.3 and 2.9 N·m during Process I and Process II, respectively. Consequently, the cutting forces and torques in CFRP are similar, regardless of the presence of Ti alloy supporting layer during drilling.

2.2 Cutting temperature

The cutting temperature of CFRP/Ti stacks during drilling is shown in Fig. 3. During Process II, the maximum cutting temperatures at the exit part of CFRP hole reaches 130.3 °C, which is about 35.5% higher than that during Process I (96.3 °C). Additionally, the cutting temperature of 8th fibre layer is 12.5% and 26.9% higher than that of 7th fibre layer during Process I and Process II, respectively. Hence, the cutting temperature is increased more with the presence of Ti alloy supporting layer.

During the drilling of CFRP/Ti stacks, CFRP and Ti alloy are almost simultaneously drilled at the interface of CFRP and Ti alloy. The change in cutting temperature at this stage is shown in zone A in Fig.3. Clearly, the two processes produce different cutting temperatures in zone A. The cutting temperature during Process II increases abruptly. Besides, the cutting temperature of Ti alloy is obtained after the drilling of 8th fibre layer, i.e., after drilling for 4.8 s.

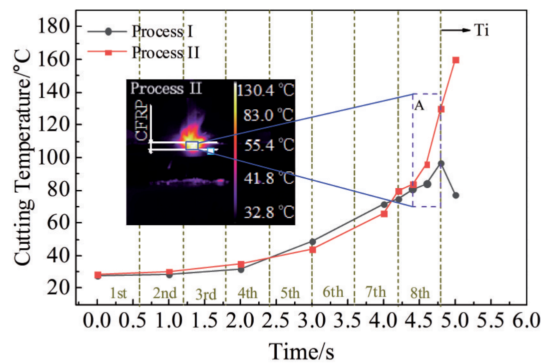

Fig.3 Cutting temperatures of CFRP drilling with and without Ti alloy supporting layer

The increased temperature in CFRP may cause changes in material properties, thus leading to serious processing damage. Excessive temperature in CFRP can easily cause the irreversible performance deterioration of the materials.

As the cutting temperature increases gradually, the internal structures of the resin molecules in CFRP and the viscoelasticity related to the internal molecular structures change greatly. Compared with the dynamic mechanical analysis results of CFRP in Ref.[22], the storage modulus of resin matrix in CFRP in Process II is almost 43%, which is lower than that in Process I, while the loss modulus is increased by 69% after Process II.

Hence, the storage modulus of the resin matrix decreases and the loss modulus increases when the processing temperature is high and almost approaches GTT, which can significantly decrease the cohesion force and rigidity of the resin matrix. Wang et al[18] found that the mechanical properties of the resin matrix change greatly when the processing temperature reaches GTT, resulting in degradation of resin and debonding of carbon fibres. Wang et al[22] analyzed the effects of HAZ on the bending performance of treated CFRP after thermal processing at different temperatures. It is reported that the bending strength declines significantly when the thermal processing temperature approaches GTT. As a result, the property of the resin matrix decreases during the processing of CFRP, and therefore the fibres cannot obtain enough support from the matrix. This phenomenon greatly influences the machining quality of CFRP, especially the surface damage.

2.3 Hole surface quality

The hole surface quality is crucial for material application. The surface morphologies of hole walls after different processes are shown in Fig. 4. The surface close to the hole entrance has high quality, while that near the hole exit is relatively inferior. The pits appear on the 8th fibre layer at the hole exit. It is difficult to observe the damage depth and to determine the fibre damage forms. Slight layering damage occurs at the hole exit after Process II. Moreover, the cutting may scratch the finished hole wall surface and thereby influence the hole quality. However, no scratches can be observed on the hole wall after Process II. In general, the hole walls after different drilling processes show the similar quality with serious damage at 8th fibre layer.

2.4 Hole subsurface quality

The fibre orientation angles in different layers are shown in Fig. 5a. A planar graph of the 8th fibre layer is presented in Fig. 5b, where θ is the included angle between the cutter movement direction and the fibre orientation, namely the cutting angle. The cutting angles of other fibre layers were measured by the similar method. Because of the anisotropism feature in fibre performance, the cutting angles have important impacts on fibre damage forms. Therefore, the subsurface damage is observed at four typical cutting angles (θ=0°, 90°, 45°, 135°) on each fibre layer.

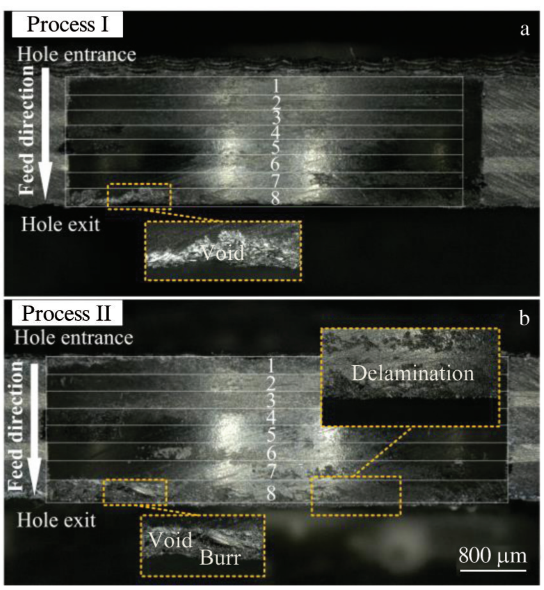

Fig.4 Surface morphologies of hole walls after Process I (a) and Process II (b)

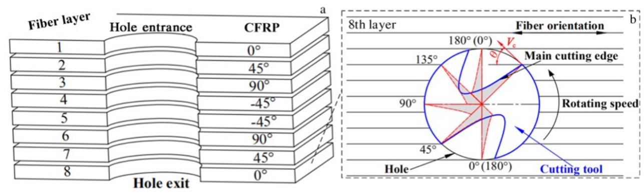

Fig.5 Schematic diagrams of fibre orientation angles (a) and cutting angle θ (b) with cutting position on the 8th fibre layer

The subsurface damage degree on the 8th fibre layer is relatively serious, as shown in Fig. 6. At the cutting angle of 0° , different degrees of transverse fibre ruptures on the subsurface of hole walls after different processes can be observed. The damage range on subsurface of hole walls after Process II is greater than that after Process II, because the tip and flank surface of the cutter can squeeze the fibres on the processed surface during drilling. Hence, the fibres on the treated surface will be bent and the elastic rebounding will also be generated[23]. Nevertheless, due to the temperature increase in fibre layer at the hole exit, the strength of the matrix is decreased. As a result, the fibres are crushed by the cutter and then fall off. The transverse pits appear on the hole surface.

Serious damage is generated on the subsurface at cutting angle of 135°. The largest subsurface damage depth is 39.1 μm after Process I. The maximum crack depth on the subsurface after Process II is 100.9 μm and the length is greater than 300 μm. Damage forms are mainly the bending ruptures of fibres and the ends of the ruptured fibres show a trend of diffusion into the bulk material. The rigidity and bonding strength of the matrix are decreased due to the high cutting temperature around the hole exit, which weakens the bonding between the fibres and matrix. Moreover, the bent fibres cannot obtain enough supports from the matrix, and therefore are easily broken. These failure mechanisms jointly form the relatively long bending ruptures.

At the cutting angle of 90°, the micro-cracks appear on the subsurface of hole walls after both the Process I and Process II, and the debonding damage occurs in the fibre matrix. Moreover, the fibres near the hole wall surface bend significantly. The longest micro-crack on the hole subsurface is 24.9 μm in length after Process II. The micro-cracks are caused by the extrusive bending of fibres on surfaces resulting from the pressure and stress from the circular bead of the cutter along the perpendicular direction.

At the cutting angle of 45° , the surface presents regular breakage pits. Moreover, the fibre damage after Process II is more serious than that after Process I. The maximum depths of the carbon fibre pits are 56.9 and 15.27 μm after Process II and Process I, respectively.

It can be seen from Fig.3 and Fig.4 that the surface quality of hole walls is relatively good at the 1st~7th fibre layers. The cutting temperature is low during the drilling of these layers and there are no significant differences in the damage degree among these layers. Hence, the subsurface damage caused by

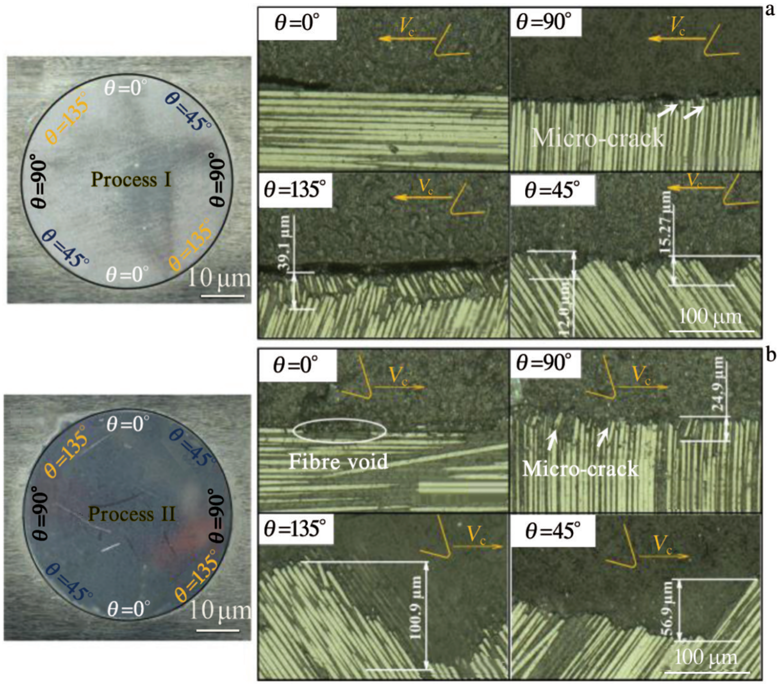

Fig.6 Subsurface damage on the 8th fibre layer of CFRP holes after Process I (a) and Process II (b)

drilling process is not very serious in these layers.

The cutting temperatures at hole exit are relatively high after Process II. Moreover, the subsurface damage on the 8th fibre layer includes serious fibre debonding, bending, and cracks. Nevertheless, the cutting temperatures at hole exits after Process I are lower than that after Process II, and the subsurface damage is also significantly less inferior. Pecat et al[24] reported the similar results that the matrix cannot effectively support fibres after thermal damage, thus resulting in broken fibres on the subsurface of the processed region. As a result, Ti alloy supporting layer mainly influences the cutting temperatures in the drilling zone of CFRP/Ti stacks, thus affecting CFRP surface quality and decreasing the structural integrity.

During the drilling of CFRP and CFRP/Ti stacks, the fibres and resin matrix primarily tolerate the stresses along the direction perpendicular to the fibre orientation and along the fibre orientation, namely Orientation 2 and Orientation 1, respectively.

When the stress is along Orientation 1, the longitudinal deformation per unit volume of fibre and resin is as follows:

$$\Delta l = \overline{\varepsilon_1}\, l \tag{1}$$

where $\overline{\varepsilon_1}$ is the average strain along Orientation 1; l is the longitudinal length.

The average stress along Orientation 1 is as follows:

$$\overline{\sigma_1} = E_1 \varepsilon_1 \tag{2}$$

where E_1 is the elasticity modulus along Orientation 1; ε_1 is the strain along Orientation 1.

Then the elasticity modulus along Orientation 1 can be expressed as follows:

$$E_1 = E_f c_f + E_m (1 - c_f) \tag{3}$$

where E_f is the fibre elasticity modulus; E_m is the matrix elasticity modulus; c_f is the carbon fibre volume fraction. E_m is decreased with increasing the temperature, leading to decrease in E_1. The strain is increased because the average stress on the fibre matrix along Orientation 1 remains constant, thus leading to the increase in Δl, which indicates that due to the reduction in elasticity modulus E_m, the deformation of the fibre matrix is increased caused by the stress along Orientation 1. Therefore, it is easy to cause micro-cracks on the subsurface.

When the stress is along Orientation 2, the transverse deformation per unit volume of fibre and resin can be expressed as follows:

$$\Delta B = \overline{\varepsilon_2}\, B \tag{4}$$

where $\overline{\varepsilon_2}$ is the average strain along Orientation 2; B is the transverse deformation degree.

Then average strain along Orientation 2 can be obtained from Eq.(5), as follows:

$$\overline{\varepsilon_2} = \overline{\sigma_2}\left(\frac{c_f}{E_f} + \frac{c_m}{E_m}\right) \tag{5}$$

where c_m is the volume fraction of the matrix; $\overline{\sigma_2}$ is the average stress along Orientation 2. The stress is increased with decreasing E_m, when the average stress along Orientation 2 remains constant, resulting in the increase in the lateral deformation. In brief, the stresses along Orientation 2 are produced through the decline in E_m, and therefore the deformation of the fibre matrix is increased. Thus, the pits and bending/broken cracks are easily generated on the subsurface.

CFRP consists of fibre and resin matrix. The resin performance directly influences the CFRP performance. High temperatures can significantly decrease the rigidity and cohesiveness of resin, thus decreasing the strength of CFRP. Due to the cutting forces, the resin performances along the directions parallel or perpendicular to the fibre orientation are decreased, resulting in the formation of micro-cracks, transverse fibre pits, continuous pits, and fibre bending ruptures on the subsurface.

2.5 Subsurface damage distribution law on fibre layers of CFRP

The distributions of subsurface damage of CFRP fibre layers were investigated layer by layer. The results show that the damage degree of the 1st~4th layers is consistent with that of the 5th layer. Thus, the damage distribution of the 1st~4th layers can be represented by that of the 5th layer. The subsurface damage positions are divided according to the cutting angles. Fig.7 presents the subsurface damage distribution on the 5th~8th fibre layers around the exit part of holes.

In Fig.7, it is clear that the maximum depth of damage is decreased with extending the distance to the hole exit. The most serious fibre damage occurs at cutting angel of 135°, and the second most severe damage occurs at cutting angel of 45°. The damage extent declines greatly at cutting angles of 0° and 90°, and the hole wall subsurface is of high quality.

2.6 Subsurface quality evaluation of hole walls

The existing methods for damage evaluation of CFRP mainly focus on damaged surfaces, the surface quality of hole walls[21,25], and the quality at the entrances and exits of holes[26]. However, they cannot provide assessment of the subsurface damage degree of CFRP. Thus, a new evaluation method is proposed in this research.

The subsurface damage can be evaluated by the sum of subsurface damage depths in fibres at each cutting angle. The calculation equation for the degree of subsurface damage S can be expressed as follows:

$$S = \sum_{i=1}^{n} d_i \tag{6}$$

where d_i is the damage depth at i layer of a certain cutting angle; n is the number of different cutting angles. This research applied 8 cutting angles (n=8): θ=0°, 45°, 90°, 135°, 180°, 225°, 270°, 315°. Fig.8 shows the subsurface damage S of each fibre layer of CFRP after different processes.

Clearly, with shortening the distance to the hole exit, S is

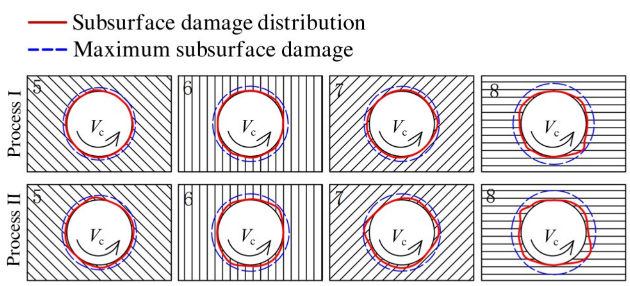

Fig.7 Damage distributions of the 5th~8th fibre layers around hole exit after different processes

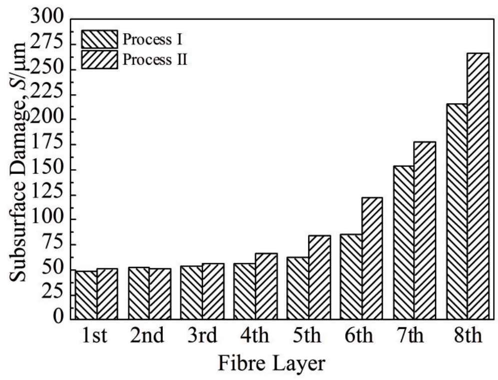

Fig.8 Subsurface damage S of each fibre layer of CFRP after different processes

increased exponentially. The damage degree of fibre layers is increased with approaching the hole exit. The subsurface damage of the 8th fibre layer is 33% and 48% higher than that of the 7th fibre layer after Process I and Process II, respectively. Moreover, the subsurface damage of the 8th fibre layer after Process II is 31% higher than that after Process I; the subsurface damage of the 7th fibre layer after Process II is 18% higher than that after Process I. Therefore, the variation in subsurface damage on fibre layers is basically consistent with that of the cutting temperature. Therefore, the subsurface damage in CFRP after Process II is worse than that after Process I.

3 Conclusions

1) During the drilling process of the carbon fibre reinforced polymer (CFRP)/Ti stacks, the cutting temperature of CFRP with Ti alloy supporting layer is 35.5% higher than that of CFRP without Ti alloy supporting layer. The presence of Ti alloy supporting layer significantly influences the cutting temperature, but only has slight effects on the hole surface quality.

2) The temperature rise can decrease the structural rigidity and bonding performance of the resin matrix. The subsurface damage of CFRP after drilling with Ti alloy supporting layer is worse than that without Ti alloy supporting layer. The subsurface damage of CFRP after drilling with and without Ti alloy supporting layer both declines with extending the distance to the hole exit.

3) At the cutting angle of 0° or 90°, the subsurface damage of CFRP is the least severe. The severe damage occurs at cutting angle of 45° and the greatest damage occurs at cutting angle of 135°. Moreover, at the fixed cutting angle, different cutting temperatures can cause different degrees of subsurface damage.

4) The sum of the depths of subsurface damage at different cutting angles can be used to evaluate the subsurface damage of CFRP components.

5) The CFRP surface quality can better reflect the subsurface damage. This study provides guidance to improve the processing quality of composite materials, which can

ameliorate the production of more advanced structures.

References

1 Qin X D, Wang B, Wang G F *et al. Journal of Mechanical Science and Technology*[J], 2014, 28(2): 713

2 Amini S, Baraheni M, Hakimi E. *International Journal of Lightweight Materials and Manufacture*[J], 2019, 2(4): 362

3 Turki Y, Habak M, Velasco R *et al. International Journal of Machine Tools and Manufacture*[J], 2014, 87: 61

4 Wang B, Wang Y F, Zhao H *et al. Composite Structures*[J], 2020, 252: 112 670

5 Zhang D W, Zhang Q, Fan X *et al. Rare Metal Materials and Engineering*[J], 2018, 47(12): 3686

6 Zhang L F, Wang S, Qiao W L *et al. The International Journal of Advanced Manufacturing Technology*[J], 2020, 106(3): 1005

7 Raj D S, Karunamoorthy L. *Materials and Manufacturing Processes*[J], 2016, 31(5): 587

8 Romoli L, Lutey A H A. *Journal of Manufacturing Processes*[J], 2019, 40: 16

9 Wang B, Gao H, Cao B *et al. Proceeding s of the Institution of Mechanical Engineers, Part B: Journal of Engineering Manufacture*[J], 2014, 228(7): 698

10 Wang Fuji, Cheng De, Zhao Meng *et al. Acta Materiae Compositae Sinica*[J], 2019, 36(2): 410 (in Chinese)

11 Xu J Y, Li C, Chen M *et al. Materials and Manufacturing Processes*[J], 2019, 34(10): 1182

12 Geng D X, Zhang D Y, Teng Y D *et al. Procedia CIRP*[J], 2018, 71: 128

13 Luo B, Zhang K F, Liu S N *et al. Chinese Journal of Aeronautics*[J], 2019, 32(9): 2211

14 Xu J Y, El Mansori M, Voisin J *et al. Journal of Manufacturing Processes*[J], 2019, 44: 435

15 Tsao C C, Hocheng H. *International Journal of Machine Tools and Manufacture*[J], 2005, 45(11): 1261

16 Hrechuk A, Bushlya V, StAhl J. *Composite Structures*[J], 2018, 204: 378

17 Jia Z Y, Chen C, Wang F J *et al. Journal of Materials Processing Technology*[J], 2020, 282: 116 665

18 Wang C Y, Chen Y H, An Q L *et al. International Journal of Precision Engineering and Manufacturing*[J], 2015, 16(8): 1689

19 Sorrentino L, Turchetta S, Bellini C. *Composite Structures*[J], 2017, 168: 549

20 Fu R, Jia Z Y, Wang F J *et al. International Journal of Machine Tools and Manufacture*[J], 2018, 135: 24

21 Wang B, Chang K, Wang M H *et al. The International Journal of Advanced Manufacturing Technology*[J], 2018, 99(5-8): 1449

22 Wang B, Yang B, Wang M H *et al. Science and Engineering of Composite Materials*[J], 2019, 26(1): 394

23 An Q L, Cai C Y, Cai X J *et al. Composite Structures*[J], 2019, 230: 111 441

24 Pecat O, Rentsch R, Brinksmeier E. *Procedia CIRP*[J], 2012, 1: 466

25 Ramirez C, Poulachon G, Rossi F *et al. Procedia CIRP*[J], 2014, 13: 163

26 Kumar D, Gururaja S. *Optics and Laser Technology*[J], 2020, 126: 106 130

钻孔过程中切削温度对CFRP亚表面的影响

王　奔[1]，王禹封[2]，赵　华[2]，王明海[1]

(1. 沈阳航空航天大学 机电工程学院，辽宁 沈阳 110136)

(2. 沈阳航空航天大学 航空制造工艺数字化国防重点学科实验室，辽宁 沈阳 110136)

摘　要：研究了碳纤维增强聚合物(CFRP)/Ti叠层构件钻孔时切削温度对钻孔质量的影响，分析了有无钛合金支撑层制孔时CFRP的切削力、切削热、孔壁表面和亚表面质量，并提出了亚表面损伤评价方法。结果表明，钻孔时钛合金支撑层对CFRP切削力及表面质量的影响较小，但对切削温度和亚表面质量影响显著。刀具同时加工钛合金和CFRP时会产生大量切削热，导致CFRP孔出口处温度大幅升高，高温导致CFRP树脂基体的刚度和粘结性能下降，使得CFRP孔出口附近纤维层上出现了严重的亚表面损伤。同时，采用提出的亚表面损伤评价方法对亚表面损伤进行评价，发现靠近出口处的纤维层亚表面损伤最为严重。在远离出口平面的方向上，亚表面损伤程度逐渐降低。因此，CFRP/Ti叠层构件钻孔过程中切削温度显著影响CFRP孔的亚表面质量，且亚表面的损伤程度是评价CFRP加工质量的重要因素。

关键词：钻孔；CFRP/Ti叠层构件；亚表面质量；温度；损伤评价

作者简介：王　奔，男，1984年生，博士，教授，沈阳航空航天大学机电工程学院，辽宁 沈阳 110136，电话：024-89728447，E-mail：wangben211@163.com